Piecemeal Microautophagy of Nucleus in *Saccharomyces cerevisiae*

Paul Roberts*† Sharon Moshitch-Moshkovitz,*† Erik Kvam*
Eileen O'Toole,‡ Mark Winey‡§ and David S. Goldfarb*

*Department of Biology, University of Rochester, Rochester, New York 14627; ‡Boulder Laboratory for Three-Dimensional Fine Structure, University of Colorado, Boulder, Colorado 80309-0347; and §Department of Molecular, Cellular, and Developmental Biology, University of Colorado, Boulder, Colorado 80309-0347

Nucleus-vacuole (NV) junctions in *Saccharomyces cerevisiae* are formed through specific interactions between Vac8p on the vacuole membrane and Nvj1p in the nuclear envelope. Herein, we report that NV junctions in yeast promote *p*iecemeal *m*icroautophagy of the *n*ucleus (PMN). During PMN, teardrop-like blebs are pinched from the nucleus, released into the vacuole lumen, and degraded by soluble hydrolases. PMN occurs in rapidly dividing cells but is induced to higher levels by carbon and nitrogen starvation and is under the control of the Tor kinase nutrient-sensing pathway. Confocal and biochemical assays demonstrate that Nvj1p is degraded in a PMN-dependent manner. PMN occurs normally in *apg7*-Δ cells and is, therefore, not dependent on macroautophagy. Transmission electron microscopy reveals that portions of the granular nucleolus are often sequestered into PMN structures. These results introduce a novel mode of selective microautophagy that targets nonessential components of the yeast nucleus for degradation and recycling in the vacuole.

INTRODUCTION

Autophagy functions in dividing cells to recycle the cytoplasm and is essential for cell viability during extended periods of starvation (Klionsky and Ohsumi, 1999). Autophagy in yeast and mammals occurs by various modes, including morphologically distinct macro- and microautophagic pathways. Macroautophagy in *Saccharomyces cerevisiae* is induced by starvation and involves the formation of double membrane autophagosomes around bulk cytoplasm and organelles (Takeshige *et al.*, 1992; Baba *et al.*, 1994). Vesicular targeting factors mediate the fusion of the outer autophagosomal membrane with the vacuole (Darsow *et al.*, 1997; Sato *et al.*, 1998), and an autophagic body is subsequently released into the vacuole lumen (Baba *et al.*, 1994) where it is degraded by acid hydrolases (Jones *et al.*, 1997). Most vacuolar hydrolases are synthesized as inactive proenzymes,

which are activated in the vacuole by Pep4p and Prb1p proteinases. Thus, autophagic bodies accumulate in the vacuoles of *pep4* or *prb1* mutant cells (Takeshige *et al.*, 1992; Woolford *et al.*, 1993; Baba *et al.*, 1994; Jones *et al.*, 1997) due to their slower degradation rates (Jones *et al.*, 1982; Zubenko *et al.*, 1983).

Many of the factors necessary for the formation of autophagosomes are used in the cytosol-to-vacuole targeting (Cvt) of proaminopeptidase I to the vacuole lumen (Scott *et al.*, 1996; Teter and Klionsky, 2000). *APG/AUT/CVT* genes, which are required for the formation of Cvt vesicles and their conversion into larger autophagosomes (Abeliovich *et al.*, 2000; Kim *et al.*, 2001a), also comprise components of a novel system of ubiquitin-like conjugation reactions (Klionsky and Ohsumi, 1999). Common to these reactions is Apg7p, a conserved E1-like enzyme (Mizushima *et al.*, 1998a,b) that is required both for the conjugation of Apg12p to Apg5p and of Aut7p/Apg8p to phosphatidylethanolamine (Ichimura *et al.*, 2000). Recently, it was shown that some Apg proteins, including Apg5p and Aut7p/Apg8p, are required for early steps in the formation of autophagosomes (Kim *et al.*, 2001b; Suzuki *et al.*, 2001; Noda *et al.*, 2002).

Inroads into the ultrastructure and genetics of microautophagy have been made in the methylotrophic yeast *Pichia pastoris*, which degrades its peroxisomes by either macro- or microautophagy (pexophagy), depending on specific meta-

bolic cues (Tuttle and Dunn, 1995; Sakai *et al.*, 1998; Hutchins *et al.*, 1999; Yuan *et al.*, 1999). Microautophagy involves the sequestration of bulk cytoplasm or organelles into the vacuolar lumen although invagination of the vacuole membrane. Scission of the invaginated vacuole membrane releases a microautophagic vesicle into the lumen where it is degraded by soluble hydrolases. The in vitro formation of microautophagic vesicles occurs independent of known factors for vacuolar fusion and vesicular trafficking (Sattler and Mayer, 2000).

VAC8 encodes a multifunctional armadillo domain protein that was originally identified in a screen for genes required for vacuole inheritance (Wang *et al.*, 1996; Fleckenstein *et al.*, 1998; Pan and Goldfarb, 1998; Wang *et al.*, 1998). Vac8p is required for vacuole-vacuole fusion (Wang *et al.*, 1998; Veit *et al.*, 2001) and Cvt targeting (Pan and Goldfarb, 1998; Wang *et al.*, 1998), but has a lesser role in macroautophagy (Pan *et al.*, 2000; Scott *et al.*, 2000). The role of Vac8p in Cvt targeting and macroautophagy is probably mediated through its interaction with Apg13p, which functions as an enhancer of Apg1p kinase activity (Noda and Ohsumi, 1998; Pan and Goldfarb, 1998; Scott *et al.*, 2000). Apg1p also mediates the induction of autophagy by the Tor signaling pathway (Hardwick *et al.*, 1999; Kamada *et al.*, 2000). Vac8p additionally plays a structural role in nucleus-vacuole (NV) junctions, which are Velcro-like patches formed through direct physical interactions between Vac8p on the vacuole membrane and Nvj1p in the outer nuclear membrane (Pan and Goldfarb, 1998). NV junctions are present in cells at all stages of the yeast cell cycle and are not required for vacuole inheritance or Cvt targeting. Two membrane proteins with roles in lipid biosynthesis, Tsc13p (Kohlwein *et al.*, 2001), a putative enoyl reductase, and Osh1p (Levine and Munro, 2001), an oxysterol binding protein, both concentrate in the NV junction-associated endoplasmic reticulum. An ankyrin repeat domain has been reported to target Osh1p to NV junctions (Levine and Munro, 2001).

Herein, we report that Vac8p and Nvj1p at NV junctions mediate a novel form of selective microautophagy aimed at degrading and recycling nonessential portions of the nucleus. During *piecemeal microautophagy of the nucleus* (PMN), small teardrop-shaped portions of the nucleus are engulfed by the vacuole. PMN is induced by nutrient limitation and by rapamycin, an inhibitor of the Tor signaling pathway. Finally, Nvj1p-enhanced yellow fluorescent protein (EYFP) is degraded by PMN in a bona fide microautophagic process that occurs independently of Apg7p and macroautophagy.

MATERIALS AND METHODS

Yeast Strains, Plasmids, and Growth Conditions

Yeast strains used in this study were YEF473a (*MAT***a**) or YEF473α (*MAT*α), (*trp1-Δ63 leu2-Δ1 ura3-52 his3-Δ200 lys2-801*), BY4741 (*MAT***a** *his3-Δ1 leu2-Δ met15-Δ ura3-Δ*) (#Y00000; Euroscarf, Frankfurt, Germany), BY *pep4-Δ* (*MAT***a** *his3-Δ1 leu2-Δ met15-Δ ura3-Δ pep4::KAN*) (#2098; Research Genetics, Huntsville, AL). Deletions of *VAC8* and *NVJ1* in YEF473α cells were described previously [Pan and Goldfarb, 1998 #8; Pan *et al.* 2000). Plasmids for expression of *NVJ1* and *NVJ1*-EYFP under *CUP1* promoter control (P_{CUP1}-*NVJ1* and P_{CUP1}-*NVJ1*-EYFP), and the construction of an integrated c*NVJ1*-EYFP gene was also described previously (Pan *et al.*, 2000). An *Eco*RI-*NVJ1*-EYFP-*Xho*II fragment was generated from P_{CUP1}-

NVJ1-EYFP by polymerase chain reaction and ligated into pYES2 (Invitrogen, Carlsbad, CA) to express Nvj1p-EYFP under *GAL1* promoter control (P_{GAL1}-*NVJ1-EYFP*). Deletions of *PEP4* and *APG7* in YEF473a cells were obtained by replacing the genes with a kanamycin resistant marker cassette as described previously (Guldener *et al.*, 1996; Wach, 1996). Cells were cultured in standard YPD and synthetic complete (SC) media (Sherman, 1991) with or without 2% glucose (SCGlu or SC-Glu, respectively) at 30°C. To induce P_{GAL1}-Nvj1p-EYFP expression, cells were cultured overnight in SC media with 2% raffinose (SCRaf) and then supplemented with 2% galactose for 3 h. Nitrogen starvation medium (SD-N) (Sherman, 1991) contained 0.17% yeast nitrogen base and 2% glucose without amino acids or ammonium sulfate.

Quantitative Degradation Analysis of Nvj1p-EYFP

Cells harboring P_{GAL1}-*NVJ1-EYFP* were grown overnight in SCRaf and subsequently diluted to an OD_{600} of ~0.5. Nvj1-EYFP expression was induced upon addition of 2% galactose to the media. After 3 h of induction, 25 OD units of culture were collected by centrifugation, washed three times with distilled water, and inoculated within 125-ml flasks into 50 ml of SD-N containing 2% glucose. Two OD units of culture were collected at 0, 2, 4, 6, 8, 10, and 20 h postinduction. Protein extracts were prepared by lysing the cells in 0.25 M NaOH, 1% β-mercaptoethanol for 10 min on ice, followed by trichloroacetic acid precipitation. Pellets were washed twice with acetone, resuspended in 25 μl of cracking buffer (8 M urea, 5% SDS, 5% β-mercaptoethanol) per OD unit, and incubated for 20 min at 72°C. Samples were separated by SDS-PAGE on 8% polyacrylamide gels and transferred onto 0.45-μm Immobilon-P membranes (Millipore, Bedford, MA). Nvj1p-EYFP was probed by immunoblot by using polyclonal anti-GFP antisera (Santa Cruz Biotechnology, Santa Cruz, CA) and detected with horseradish peroxidase-coupled donkey anti-rabbit antibody (Santa Cruz Biotechnology). Horseradish peroxidase activity was monitored by chemiluminescence by immunoblot with Luminol reagent (Santa Cruz Biotechnology). The average pixel intensity of Nvj1p-EYFP present in each extract was quantified from a digital scan by using NIH Image 1.62 (a public domain program developed at the National Institutes of Health and available on the Internet at http://rsb.info.nih.gov/nih-image/). Average pixel intensities were normalized according to a nonspecific band on the immunoblot and multiplied by the ratio of cell growth over the 20-h period using OD_{600} measurements.

Confocal Analysis of NV Junctions and PMN Structures

PMN structures were visualized using c*NVJ1*-EYFP expressed from its native promoter in the chromosome or from a plasmid (P_{CUP1}-*NVJ1*-EYFP). Basal levels of P_{CUP1}-*NVJ1*-EYFP expression in YPD or SCGlu were achieved by withholding exogenous Cu^{2+}. Higher levels were achieved by adding 0.1 mM $CuSO_4$ for the times indicated. Vacuoles were stained with *N*-[3-triethylammoniumpropyl]-4-[*p*-diethylaminophenylhexatrienyl] pyridinium dibromide (FM4-64) as described previously (Pan *et al.*, 2000). If cells were to be starved for nitrogen (SD-N) or glucose (SC-Glu) before imaging, they were first stained with FM4-64, and then washed 5× in SD-N or SC-Glu and resuspended in SD-N or SC-Glu media for 3 h. DNA was stained immediately before imaging with 5 μM Hoechst reagent H-1398 (Molecular Probes, Eugene, OR) in SCGlu or SD-N. For rapamycin treatment, cells in SCGlu were treated for 3 h with a final concentration of 0.2 μg/ml rapamycin by using a stock solution of 20 μg/ml rapamycin (Calbiochem, San Diego, CA) in 90% ethanol/10% Triton X-100. Control cells were treated with the same volume of the ethanol/Triton X-100 buffer without rapamycin.

Confocal Microscopy

Confocal microscopy was performed on a Leica TCS NT microscope (Carl Zeiss, Thornwood, NY) equipped with UV, Ar, Kr/Ar, and

He/Ne lasers. Images were processed using MetaMorph (Universal Imaging, Downington, PA) or PhotoShop 5.0 (Adobe Systems, Mountain View, CA).

Cryofixation Electron Microscopy and Three-Dimensional Reconstruction

Cells were grown for 3 h in SD-N then prepared for electron microscopy by using methods described previously (Winey *et al.*, 1995). Briefly, cells were collected by vacuum filtration onto a 0.45-μm filter (Millipore), the cell paste quickly transferred into freezing hats, and the samples frozen in a Balzer's HPM010 high-pressure freezer (Bal-Tec, Liechtenstein). The frozen cells were freeze-substituted in 2% OsO_4 and 0.1% uranyl acetate in acetone for 3 d at $-90°C$, and then warmed to room temperature and embedded in Epon-Araldite for routine microscopy. Serial 70-nm-thick sections were cut using a Reichert-Ultracut-E microtome (Leica Microsystems, Deerfield, IL) and collected onto formvar-coated copper slot grids. Sections were poststained with 2% aqueous uranyl acetate followed by lead citrate.

The serial sections were imaged in a CM10 electron microscope (Philips Electronic Instruments, Mahwah, NJ) operating at 80 kV. Serial images were collected through PMN structures by using a GATAN charge-coupled device camera mounted on the microscope. The digital images were then aligned, and the nuclear envelope, nuclear pores, nucleolus, and vacuole membranes were modeled and displayed using the IMOD software package (Kremer *et al.*, 1996).

RESULTS

Surface Area of NV Junctions Increases in Response to Nutrient Limitation

The *NVJ1* promoter contains two stress response element consensus sequences (Moskvina *et al.*, 1998), and *NVJ1* mRNA levels correspondingly increase under conditions of nitrogen limitation (Gasch *et al.*, 2000) as well as after the diauxic shift (DeRisi *et al.*, 1997). We monitored the frequency and morphology of NV junctions as a function of culture density by using cNvj1p-EYFP as a reporter. *cNVJ1*::EYFP was created by integrating EYFP downstream of chromosomal *NVJ1* (Pan *et al.*, 2000) to generate an Nvj1p-EYFP reporter under the control of the native *NVJ1* promoter. cNvj1p-EYFP fluorescence localized exclusively to NV junctions and colocalized with FM4-64–stained vacuolar membranes. In early log phase, ~50% of cells contained detectable NV junctions (Figure 1). Many of the NV junctions in early log phase cells appeared as small dots rather than lines or patches. Thus, a small percentage of NV junctions may have been too tiny or dim to detect by confocal microscopy. At higher cell densities, the surface areas of individual NV junctions increased and the percentage of NV junction-positive cells grew to >90%. The sizes and frequencies of NV junctions also increased after switching early log phase cultures to nitrogen (SD-N) or carbon (SC-Glu) starvation media (our unpublished data). The expansion of NV junctions in late log-phase or depleted media suggests that NV junctions play a role in the cell's response to nutrient limitation.

Nuclear Envelope Blebbing in Context of NV Junctions

NV junctions usually appear as smooth curvilinear stripes (Pan *et al.*, 2000). Infrequently, however, NV junction-asso-
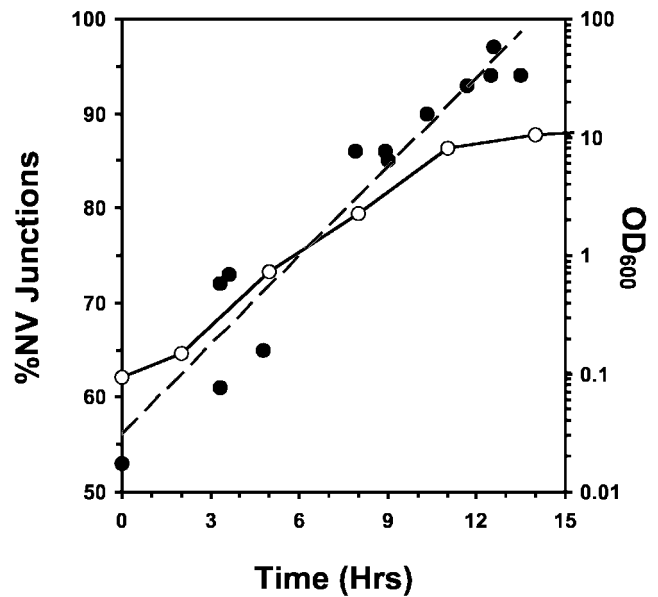

Figure 1. Frequencies of NV junctions increase during growth in rich medium. The percentage of c*NVJ1*::EYFP YEF473a cells containing cNvj1p-EYFP–stained NV junctions (filled circles, dashed gray line) as a function of growth in YPD (open circles, black line). At least 100 cells were scored for junctions at each point.

ciated nuclear envelopes were contorted into convex bulges and teardrop-like blebs that protruded into the vacuole membrane (Figure 2A). Although the transmission electron microscopy (TEM) images in Figure 2A were taken from *NVJ1*-overexpressing cells, similar structures occurred in normal cells as well (see below).

Nuclear bulges and blebs such as those shown in Figure 2A were always observed in association with vacuoles. The morphology of these structures suggested that the nucleus might be subject to microautophagy. This notion was investigated by examining the morphology of NV junctions in nitrogen starvation medium (SD-N). Experiments were performed in starved *pep4-Δ* cells to promote the accumulation of autophagic vesicles (Takeshige *et al.*, 1992; Baba *et al.*, 1994). Vesicles originating from NV junctions were observed using P_{CUP1}-Nvj1p-EYFP as a fluorescent reporter because previous studies demonstrated that this functional reporter concentrates into NV junctions (Pan *et al.*, 2000). Figure 2B shows the localization of Nvj1p-EYFP (a) and FM4-64–stained vacuoles (b) in two cells that exhibit extreme nuclear envelope perturbations. Regions of colocalization at NV junctions between Nvj1p-EYFP and FM4-64 appear yellow in the overlay image (c). As a consequence of overexpression, Nvj1p-EYFP localized not only to NV junctions but to a lesser extent over the entire nuclear surface (Pan *et al.*, 2000). In the upper cell in Figure 2B, an Nvj1p-EYFP-stained bleb remained attached to the nucleus by a thin tether (see arrow, a). In the lower cell, what appears to be a free intra-vacuolar vesicle is situated across the vacuole from the nucleus. Significantly, Nvj1p-EYFP–labeled blebs and vesicles always stained with FM4-64 (Figure 2B, b). Because the FM4-64 used for vacuole labeling was washed away before the cells were shifted into SD-N medium, FM4-64–stained
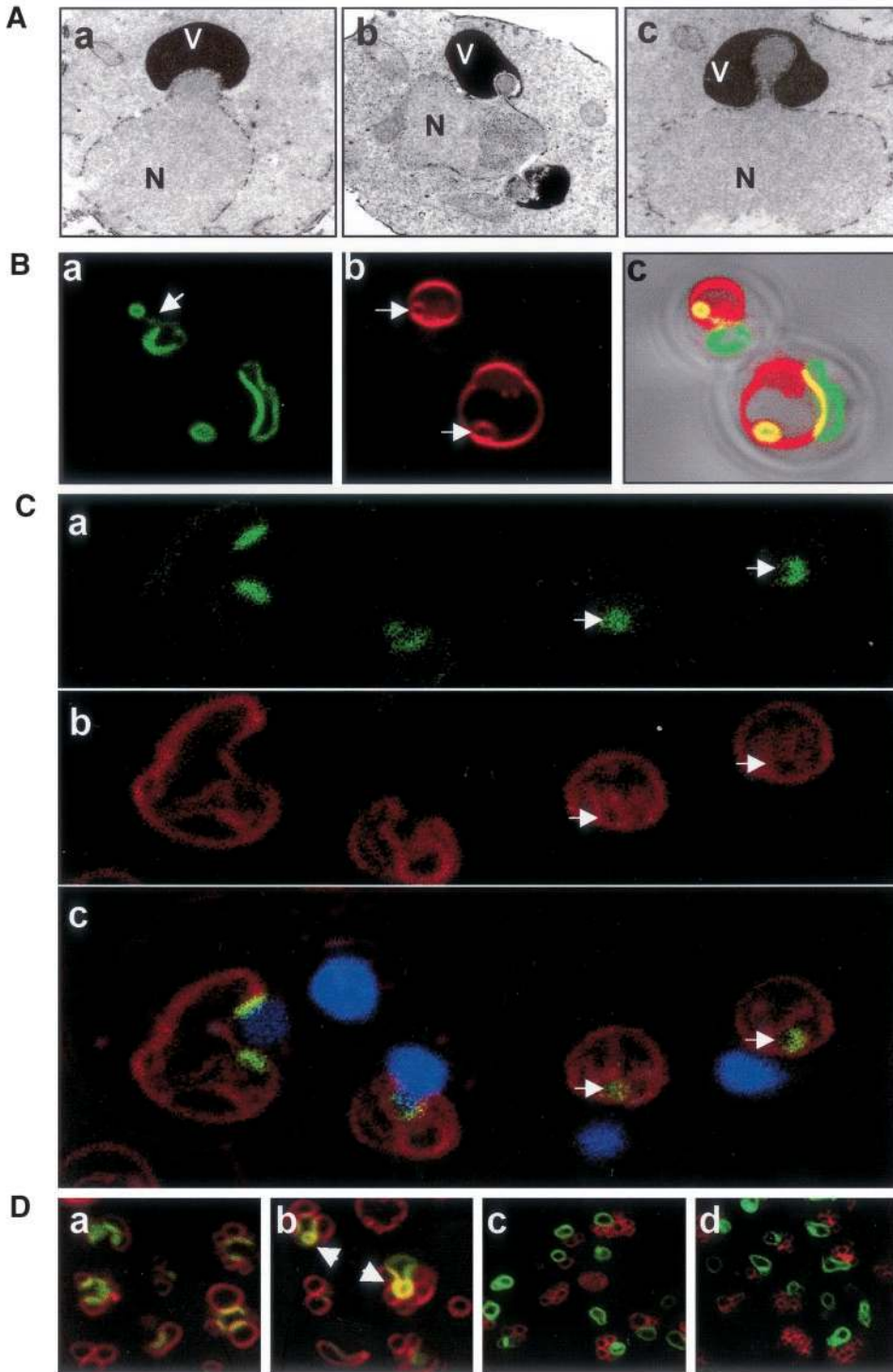
Figure 2. Vacuole-associated nuclear bulges, blebs, and intravacuolar vesicles. (A) Electron micrographs of a vacuole-associated nuclear envelope bulge (a) and blebs (b and c) (V, vacuole; N, nucleus). YEF473a cells were processed for TEM as described in MATERIAL AND METHODS. (B) Confocal images of extreme nuclear exvaginations in two starved *pep4-Δ* cells expressing P_{CUP1}-*NVJ1*-EYFP and stained with FM4-64 (see MATERIALS AND METHODS). Nvj1p-EYFP (a), FM4-64 (b), and differential interference contrast overlay (c). Arrow in a points to a thin tether connecting the intravacuolar structure to the nucleus. Arrows in b point to FM4-64–stained intravacuolar membrane vesicles. (C) Nuclear envelope blebs and vesicles in cNvj1p-EYFP–expressing cells. Images show cNvj1p-EYFP (a), FM4-64 (b), and overlay (c) of a and b with Hoechst and differential interference contrast. Arrows point to intravacuolar vesicles. (D) Nuclear envelope blebbing is dependent on Vac8p. Nvj1p-EYFP–labeled blebs and vesicles were monitored in *VAC8* (a and b) and *vac8-Δ* cells (c and d) in rich (YPD) (a and c) and starvation (SD-N) (b and d) media. Cells were grown in ScGlu, P_{CUP1}-*NVJ1:EYFP* expression induced for 1 h with 0.1 mM Cu^{2+}, stained with FM4-64, and starved for 3 h in SD-N, or incubated in YPD for the same time period, as described in MATERIALS AND METHODS. Arrows indicate PMN structures.

intravacuolar vesicles present after 3 h of starvation were likely formed through invagination of prestained vacuolar membranes. These types of structures suggest that Nvj1p-EYFP–labeled nuclear envelope vesicles were pinched off into the vacuole lumen by microautophagy. Similar structures were observed using an integrated *cNVJ1*::EYFP reporter. Blebs and vesicles produced by cells expressing either P_{CUP1}-*NVJ1*-EYFP or *cNVJ1*::EYFP were morphologically similar except for their size, which depends on *NVJ1* expression levels (Figure 2C). In contrast to P_{CUP1}-*NVJ1*-EYFP expressing cells, in which over-
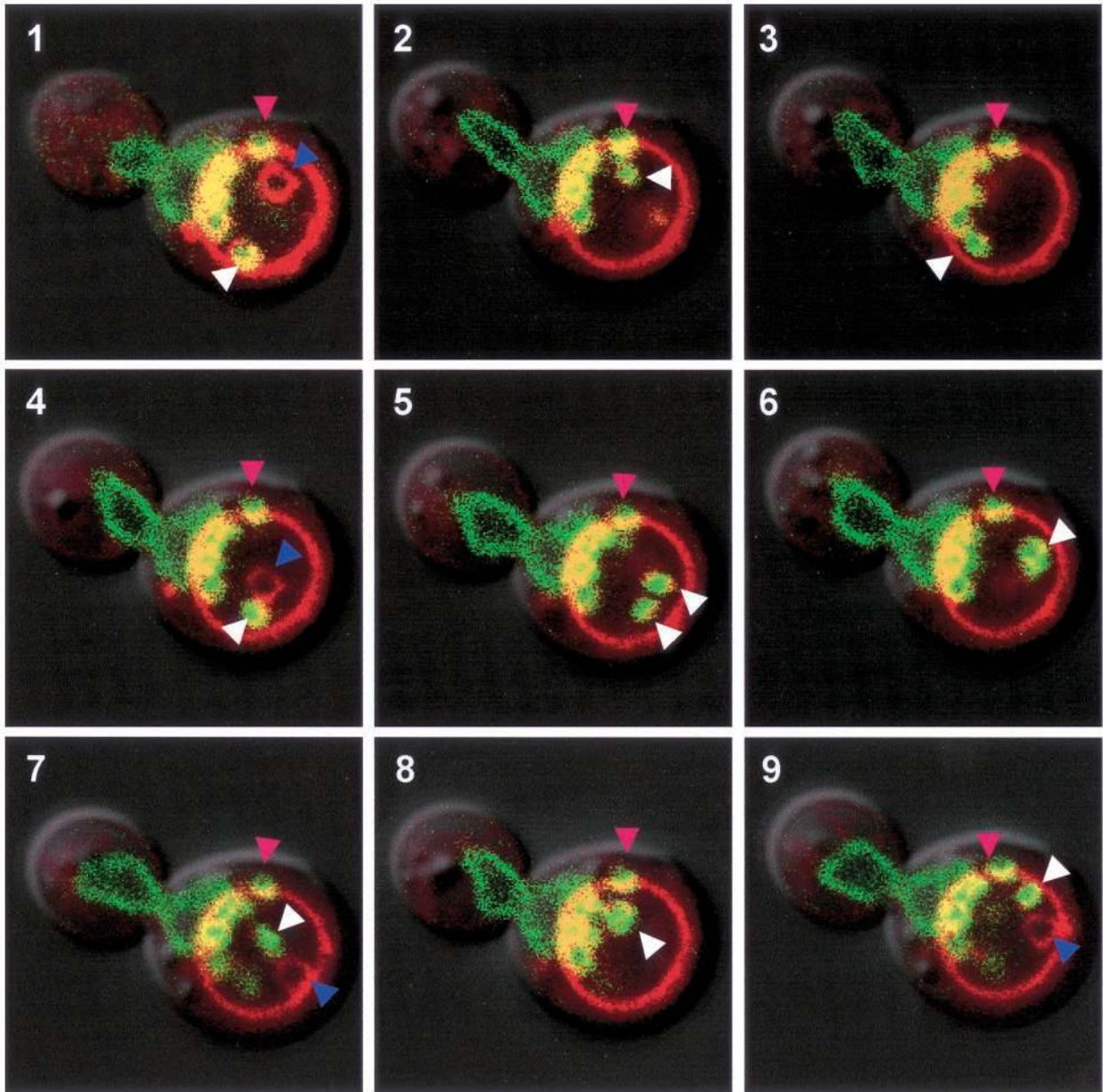
Figure 3. Movement of intravacuolar nuclear envelope vesicles. Images taken at 90-s intervals of an Nvj1-EYFP–expressing wt cell containing a number of blebs and vesicles. At least two Nvj1p-EYFP/FM4-64–stained vesicles moved freely in the vacuole (white arrowheads). An immobile Nvj1p-EYFP/FM4-64–stained bleb/vesicle located away from the NV junction but adjacent the vacuole membrane (pink arrowhead). In addition to blebs associated with the NV junction, this cell contains a mobile vesicle stained only with FM4-64 (purple arrowhead). Cells were grown in YPD, stained with FM4-64, starved for 3 h in SD-N, and stained with Hoechst as described in MATERIALS AND METHODS.

expressed Nvj1p-EYFP can encircle the nucleus (Figure 2B), cNvj1p-EYFP labeling is restricted to NV junctions (Figure 2C, a and c). Interestingly, entire NV junctions can pinch off into the vacuole in cNvj1p-EYFP cells, leaving little or no EYFP-tagged nuclear envelope behind (Figure 2C, c, arrowheads).

Autophagic vesicles that are released into the vacuole lumen display characteristically rapid Brownian motions that are readily observed by light or confocal microscopy. A time series demonstrates that Nvj1p-EYFP–labeled intravacuolar structures appear and behave like other free-floating autophagic vesicles (Figure 3). These images at 90-s intervals follow a mitotic cell stained with FM4-64 and Nvj1p-EYFP. This extraordinary cell is literally foaming with Nvj1p-EYFP–labeled vesicles, presumably from its large NV

junction into the mother cell's FM4-64–stained vacuole. In addition to nuclear envelope blebs and/or vesicles that remain closely associated with the NV junction throughout the time course, there are at least two rapidly moving Nvj1p-EYFP/FM4-64–costained vesicles that are seen in the same focal plane only once during the time course (white arrowheads, 5). Another Nvj1p-EYFP/FM4-64–stained vesicle seems to have dissociated from the NV junction but remains stuck to the vacuole membrane (pink arrowheads). Because vesicles are delivered into the vacuole lumen from multiple sources, it is not surprising to observe a rapidly moving FM4-64–stained vesicle that is not labeled with Nvj1p-EYFP (visible in 1, 4, 7, and 9, purple arrowheads).

Previously, we showed that the formation of NV junctions was dependent on both *VAC8* and *NVJ1* (Pan *et al.*, 2000). The dependence of vacuole-associated nuclear envelope blebbing and vesiculation on *VAC8* was investigated by confocal imaging of Nvj1p-EYFP– and FM4-64–stained wt and *vac8-Δ* cells. NV junctions occurred in both unstarved and starved wt cells, but were absent in *vac8-Δ* cells (Figure 2D). After 3 h in SD-N, Nvj1p-EYFP–tagged blebs and intra-vacuole vesicles were frequently detected in the population of wt cells, but not in starved *vac8-Δ* cells (Figure 2D). Blebs were also observed in dividing cells in YPD medium, albeit less frequently. Tsc13p-GFP, an integral membrane protein of the perinuclear and peripheral ER, was recently reported to accumulate in NV junctions and bleb-like structures similar to those described in this report (Kohlwein *et al.*, 2001). Using Tsc13p-GFP as a reporter, we observed that NV junctions and blebs were absent from both *vac8-Δ* and *nvj1-Δ* cells (our unpublished data). We conclude that the NV junction forming proteins Vac8p and Nvj1p are required for the production of vacuole-associated nuclear envelope blebs.

Physiological Control of Nuclear Envelope Blebbing

The results shown in Figure 1 indicate that the frequency and surface area of NV junctions increase as nutrients become depleted during asynchronous growth. We investigated whether the blebbing of NV junctions responds to nutrient limitation by counting cNvj1p-EYFP–labeled blebs and vesicles during growth in rich (YPD), nitrogen starvation (SD-N), and carbon starvation (SD-Glu) media. This assay depends on scoring cNvj1p-EYFP–associated blebs and vesicles by confocal microscopy, and does not account for variations in the relative sizes of the blebs and vesicles or variations in the relative rates of vesicle throughput. Because the aim of these experiments was to assess nuclear envelope blebbing under physiologically relevant conditions, it is important to emphasize that the cNVJ1::EYFP reporter gene is expressed from its native promoter. As shown in Figure 4A, 5–10% of cells in early log phase contained at least one bleb or vesicle. The frequency of these structures rose steadily during growth, reaching ~35% by late log/early stationary phase. Blebbing frequencies were already on the rise during early to mid-log phase growth, ". . . at a time when rRNA transcription begins to decline, when cells are still firmly in log phase, when less than a third of the glucose has been consumed, and when cell density is <20% of its final value." (Ju and Warner, 1994).

The affect of nitrogen starvation on the frequency of blebbing was assessed by transferring cells at various times from YPD to SD-N medium for 3 h before counting blebs and
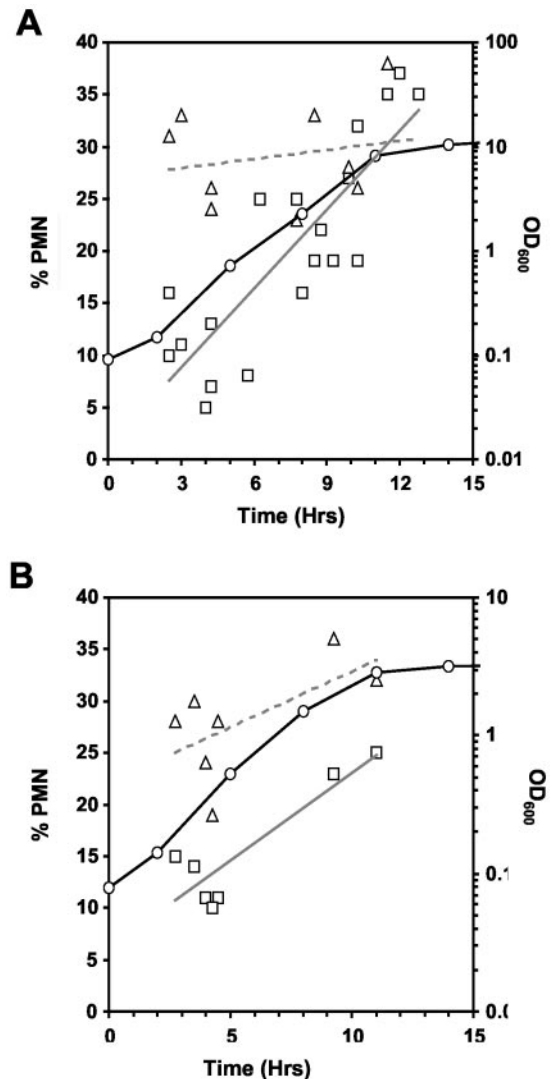

Figure 4. Physiological control of nuclear envelope blebbing. Frequencies of cNvj1p-EYFP–labeled blebs and vesicles as a function of growth, starvation, and rapamycin treatment in c*NVJ1*::EYFP YEF473a cells. (A) During growth in YPD (open circles, black line), cells at different OD_{600} were scored for vacuole-associated nuclear envelope blebs and vesicles (squares, gray regression line). Cells in YPD were transferred to SD-N medium at different times during the growth curve, and after 3 h, were scored for blebs and vesicles (triangles, dashed regression line). (B) Cells grown in SCGlu were scored for blebs and vesicles (squares, gray regression line) as a function of the growth curve (circles, black line) and after treatment with rapamycin (gray triangles, dashed regression line) as described in MATERIALS AND METHODS. At least 100 cells were scored at each point.

vesicles (Figure 4A). Because the cells were transferred directly from YPD into SD-N, early log cells did not have the opportunity to adapt gradually to nitrogen depletion. Blebbing levels rose three- to fourfold in cells taken from early log phase cultures and transferred into SD-N. However, by early stationary phase, the frequency of blebbing seemed to

have reached a steady-state maximum level (Figure 4A), and the transfer of these cells into SD-N did not further increase the frequency of blebs. Blebbing levels also rose in response to glucose starvation. In this experiment, performed in triplicate, the frequency of blebs and vesicles increased from $5 \pm 2.3\%$ in cells grown to early log phase in SCGlu ($OD_{600} = 0.235$) to $22 \pm 1.5\%$ after 3 h in SC-Glu.

Because blebs accumulate to their highest levels in exhausted media, it is possible that they signal cell death. Cell viabilities after incubation in SD-N for various times were assessed by plating onto YPD, and did not vary much from ~90% during the first several days in SD-N (our unpublished data), despite the fact that after 3 h 30–35% of the cells contained blebs and/or vesicles (Figure 4A). We conclude that nuclear envelope blebbing in the context of NV junctions is normally neither cause nor consequence of cell death.

Rapamycin inhibits Tor kinase function and induces macroautophagy in rapidly dividing cells in rich medium (Noda and Ohsumi, 1998). We investigated the affect of rapamycin on blebbing as a function of cell density in SCGlu. Similar to the effects of nitrogen and carbon starvation, the frequency of blebs/vesicles in early log cells increased about threefold in the presence of rapamycin (Figure 4B). These results indicate that the Tor nutrient response pathway controls vacuole-associated nuclear envelope blebbing.

Taken together, these results show that nuclear envelope blebbing is increasingly induced in proportion to the degree of carbon and nitrogen depletion. By analogy to macroautophagy mutants (*apg/aut/cvt*), one might expect that *nvj1-Δ* cells would be less well adapted for long-term starvation. The viabilities of *nvj1-Δ* and wt cells grown to early log phase in YPD and transferred to SD-N were monitored for 40 d by plating assay (our unpublished data). The viability of both cultures remained >75% for 16 d, after which time the cells in both cultures slowly began to die at virtually the same rate. After 40 d in SD-N only ~10% of wt and *nvj1-Δ* cells produced colonies on YPD plates. In contrast, only ~10% of *apg13-Δ* cells, which are defective in macroautophagy, remained viable after 5 d in SD-N (P. Roberts and X. Pan, unpublished data). Therefore, despite the fact that NV junctions increased in size and nuclear envelope blebs became more abundant during nutrient limitation, these phenomena are apparently not important contributors to cell survival in nitrogen starvation medium. It is possible that redundant degradation pathways operate in the absence of NV junction-mediated nuclear autophagy.

Nuclear Envelope Vesicles Are Degraded by Vacuolar Hydrolases in a Macroautophagy-independent Manner

A classical method for determining whether intravacuolar vesicles are degraded by vacuole hydrolases is to note their accumulation in hydrolase-deficient *pep4-Δ* cells (Takeshige *et al.*, 1992; Baba *et al.*, 1994; Abeliovich *et al.*, 1999). Thus, we monitored *pep4-Δ* cells to determine whether Nvj1p-EYFP-labeled nuclear envelope blebs are normally degraded. After 3 h in SD-N medium, ~30% wt and ~67% *pep4-Δ* cells contained Nvj1p-EYFP/FM4-64–stained microautophagic structures (Figure 5A). In addition, the vacuoles of *pep4-Δ* cells often contained more than one vesicle. Therefore, we

conclude that nuclear envelope blebs are pinched off into the vacuole and degraded.

Previous reports indicate that microautophagy is dependent on macroautophagy. Specifically, microautophagy of the *S. cerevisiae* cytosol is partially inhibited by mutations in several different *APG* genes (Muller *et al.*, 2000; Sattler and Mayer, 2000). Also, micropexophagy in *P. pastoris* is inhibited by mutations in *GSA7* (*APG7* in *S. cerevisiae*), which is absolutely required for macroautophagy (Yuan *et al.*, 1999). For this reason, we quantified the frequency of nuclear blebbing in *apg7-Δ* cells. After 3 h in SD-N the frequency of nuclear envelope blebs in *apg7-Δ* cells was comparable with levels observed in wt cells (Figure 5A). Figure 5B shows confocal images of starved wt, *apg7-Δ* and *pep4-Δ* cells. The morphology of the vacuoles and nuclear envelope blebs in wt and *apg7-Δ* cells was indistinguishable. These results demonstrate that the morphological intermediates of NV junction-mediated microautophagy of the nucleus occur at normal frequencies in cells that are deficient in macroautophagy.

Degradation of Nvj1p Is Dependent on Pep4p and Vac8p but Not Apg7p

The accumulation of nuclear blebs and vesicles in *pep4-Δ* cells provides indirect evidence that portions of the nucleus are normally targeted to the vacuole and degraded in both dividing and starving cells. Still, we sought direct biochemical evidence for the microautophagy of nuclear proteins. Nvj1p-EYFP is a convenient visual and biochemical marker for monitoring the vacuolar degradation of nuclear blebs since every bleb delivered to the vacuole is necessarily decorated with NV junction-associated Nvj1p. The degradation of Nvj1p-EYFP in YEF473 wt, *pep4-Δ*, *vac8-Δ*, and *apg7-Δ* cells was quantified as a function of time in nitrogen starvation medium. A pulse of Nvj1p-EYFP was initially generated by inducing P_{GAL1}-*NVJ1*-EYFP expression for 3 h by adding 2% galactose to SC raffinose medium and repressing expression by switching the cells to glucose-containing SD-N medium for the duration of a 20-h time course. As previously described, overexpression of *NVJ1* or *NVJ1*-EYFP results in the spreading of excess protein outside NV junctions and over the surface of the nuclear envelope (Pan *et al.*, 2000). The galactose induction period was limited to minimize the spreading of Nvj1p-EYFP outside NV junctions without sacrificing the sensitivity of the immunoblot analysis. Because the formation of NV junctions requires both Vac8p and Nvj1p, Nvj1p-EYFP will always spread over the surface of nuclei in *vac8-Δ* cells, regardless of its level of expression (Figure 2D, c and d).

As shown in Figure 6A, the level of Nvj1p-EYFP declined significantly during the 20-h time course in wt cells, but was stable in *pep4-Δ* cells. The lack of degradation *pep4-Δ* cells confirms that Nvj1p-EYFP is degraded in the vacuole. The kinetics of degradation of Nvj1p-EYFP in wt cells was severalfold slower than that reported for the peroxisomal marker Fox3p under similar conditions in SD-N (Hutchins *et al.*, 1999). The relatively long half-life of Nvj1p-EYFP probably reflects the fact that only a portion of each NV junction in these cells is incorporated into individual nuclear envelope blebs. Still, the kinetics of Nvj1p-EYFP degradation was significantly faster than that reported for the turnover of Golgi and mitochondrial markers in SD-N (Hutchins *et al.*,
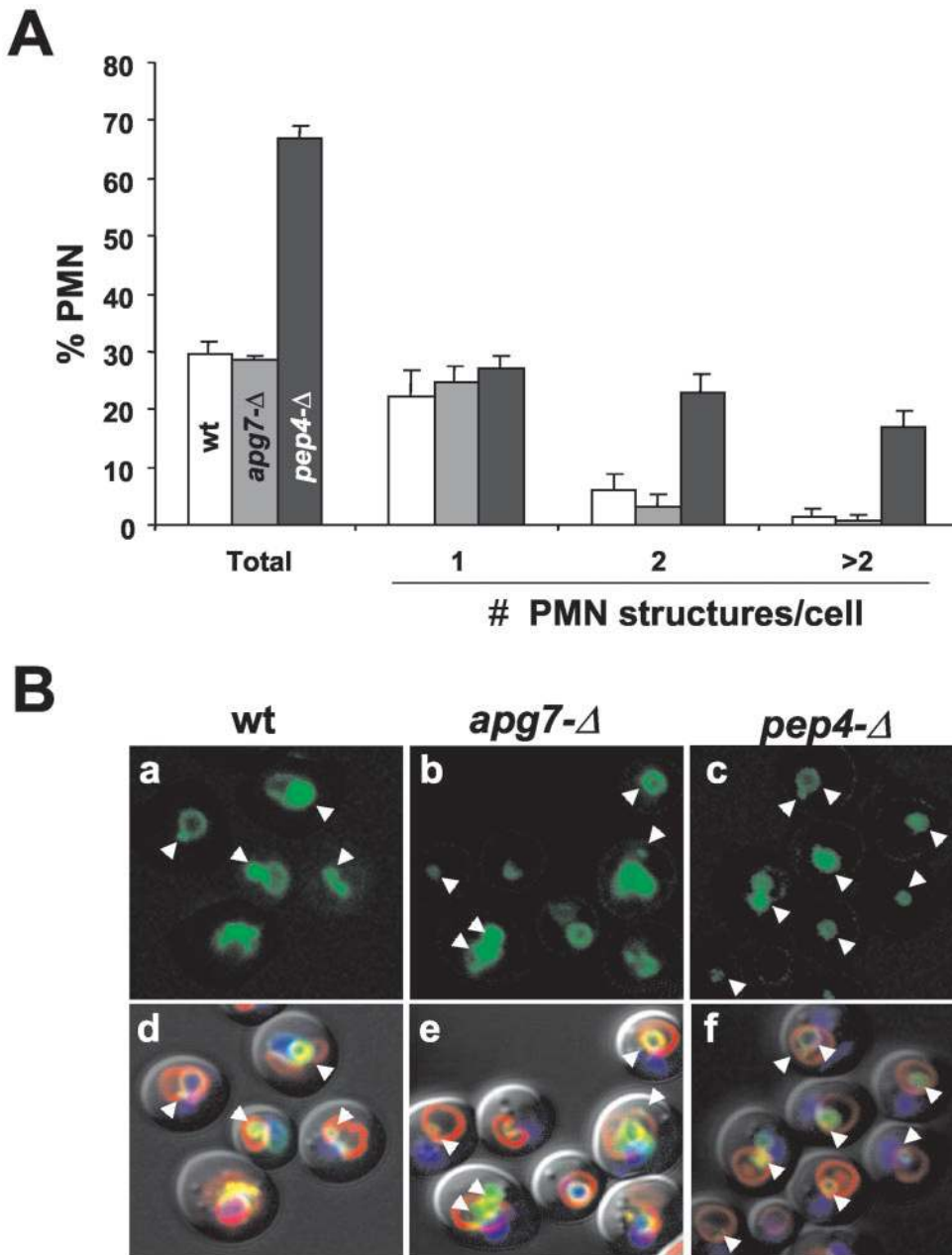
Figure 5. Degradation of nuclear envelope blebs is *PEP4*-dependent and *APG7*-independent. (A) Frequencies of Nvj1p-EYFP/FM4-64–stained nuclear envelope blebs and vesicles in wt (white bars), *apg7*-Δ (gray bars) and *pep4*-Δ (black bars) BY4741 cells. Each bar represents the mean of three independent counts of at least 100 cells. (B) Nvj1p-EYFP–labeled blebs and/or vesicles in wt, *apg7*-Δ, and *pep4*-Δ cells (arrowheads). (a–c) Cells stained with Nvj1p-EYFP (green). (d–f) Overlays of a, b, and c with Hoechst-stained chromatin (blue), FM4-64 for the vacuole membrane (red), and differential interference contrast. P_{CUP1}-*NVJ1*::EYFP expression in the indicated strains was induced for 1 h with 0.1 mM Cu^{2+}, shifted to SD-N medium for 3 h, and stained with Hoechst as described in MATERIALS AND METHODS.

1999). Nvj1p-EYFP degradation rates were also faster than the proteolytic processing of Pho8Δ 60p, an engineered cytosolic protein that serves as a marker for the nonselective delivery of cytosolic proteins to the vacuole (Noda *et al.*, 1995; Hutchins *et al.*, 1999).

Nvj1p-EYFP degradation seemed to be normal in *apg7*-Δ cells, indicating that macroautophagy does not play an important role in nuclear microautophagy. Finally, the degradation of Nvj1p-EYFP was significantly reduced in *vac8*-Δ cells. Figure 6B shows the actual extent of Nvj1p-EYFP degradation at 20 h, after normalizing the immunoblot data for sample loading and cell division factors (see MATERIALS

AND METHODS). Similar results were obtained using BY4741 wt, *pep4*-Δ, *vac8*-Δ, and *apg7*-Δ cells (our unpublished data). The small but measurable degradation of Nvj1p-EYFP observed in *vac8*-Δ cells (Figure 6B) could be due to its abnormal localization. In the absence of Vac8p, Nvj1p-EYFP spreads over the entire nuclear surface instead of concentrating into NV junctions (Pan *et al.*, 2000). Perhaps its increased exposure somehow makes the protein more susceptible to degradation by less efficient alternative mechanisms. In conclusion, these biochemical data, which are consistent with the morphological evidence presented in Figure 5, demonstrate that portions of the yeast nucleus are
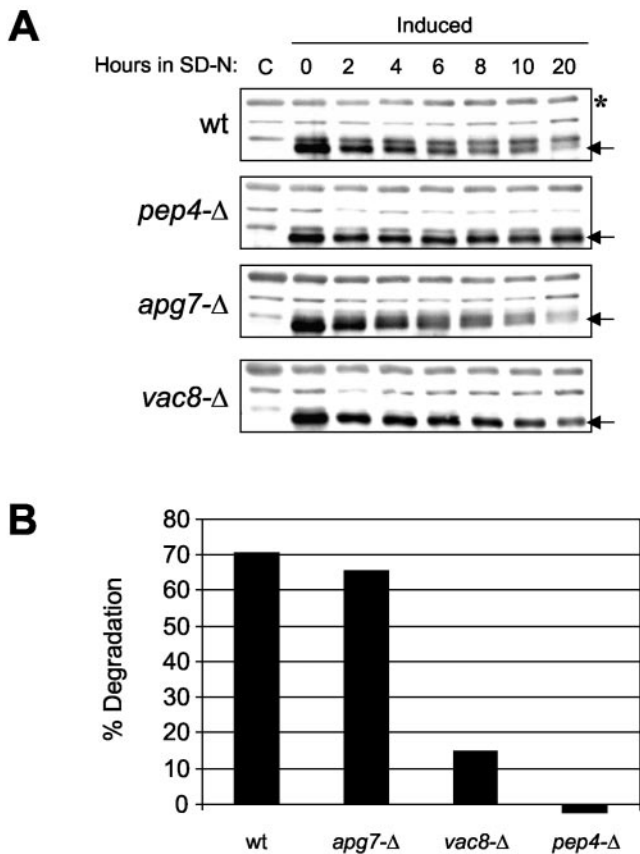
Figure 6. The degradation of Nvj1p-EYFP is dependent on Pep4p and Vac8p but not Apg7p. (A) wt, *pep4-Δ*, *vac8-Δ*, and *apg7-Δ* cells harboring P_{GAL1}-*NVJ1-EYFP* were induced to express Nvj1p-EYFP for 3 h in 2% galactose and then shifted to glucose-containing starvation media (SD-N). Two OD units of culture were collected at the indicated times postinduction. Protein extracts were prepared and Nvj1p-EYFP levels (see arrows) were analyzed by immunoblot as described in MATERIALS AND METHODS. Uninduced control extracts are denoted as C. (B) Degradation levels of Nvj1p-EYFP after 20 h in SD-N. Nvj1p-EYFP protein levels were quantified at times 0 and 20 h (see arrows) and normalized against a nonspecific band (see asterisk) and adjusted for cell growth as described in MATERIALS AND METHODS.

targeted for degradation in the vacuole by a NV junction-dependent, Apg7p-independent microautophagic process.

Portions of Nucleolus Are Frequently Partitioned into Microautophagic Nuclear Blebs

The partitioning of dense granular material into some vacuole-associated nuclear envelope blebs was readily apparent in transmission electron micrographs. The images shown in Figure 7A are of starved *myo1-Δ* cells. *myo1-Δ* cells (gift of Erfei Bi, University of Pennsylvania, Philadelphia, PA), were used because they accumulate large numbers of blebs in both dividing and starving cells (P. Roberts and D.S. Goldfarb, unpublished observations). The cell shown in Figure 7A, a–c, contains two blebs, one of which seems to be filled

with granular material from the adjacent nucleolus. Preribosomes are responsible for the characteristic morphology of the dense granular component of the nucleolus (Leger-Silvestre *et al.*, 1999). A three-dimensional reconstruction from serial thin sections of this cell shows that both nuclear blebs are fully engulfed by invaginations of the vacuole membrane (Figure 7A, d–f). Nuclear pore complexes are absence from both nuclear envelope blebs (Figure 7A, d and f), which is consistent with previous findings that pore complexes are absent from NV junctions (Severs *et al.*, 1976; Pan *et al.*, 2000). The partitioning of nucleolar material into blebs is a frequent occurrence, but many blebs emerge from regions of the nuclear envelope that are not associated with the nucleolus and do not seem to contain nucleolar material. For example, although the contents of the lower bleb in the cell shown in Figure 7A are concentrated relative to the bulk nucleoplasm, they do not seem to contain preribosomes.

Evidence that contents of the nucleoplasm can become concentrated or aggregated before or during its partitioning into nuclear envelope blebs is shown in Figure 7B. Here, highly condensed material that may or may not be of nucleolar origin appears within the neck and bulb of an elongated bleb that protrudes into a section of the vacuole containing other vesicles. It is apparent at higher magnification (Figure 7B, c) that the nuclear envelope at the base of the bleb has separated from the dense underlying chromatin. The plastic properties of the yeast nuclear envelope are highlighted by the capacity of the bleb in this cell to span the relatively wide separation between the nucleus proper and the vacuole. Yeast nuclei do not contain the fibrous nuclear lamina network that confers rigidity to the nuclei of higher cells.

DISCUSSION

The results presented herein indicate that portions of the *S. cerevisiae* nucleus are targeted for degradation and recycling by a novel form of selective microautophagy. Because small pieces of the nucleus are sequestered into invaginations of the vacuolar membrane and subsequently degraded, we call this process PMN. Figure 7C shows a model of PMN that incorporates five morphologically distinct intermediates as revealed by confocal and electron microscopy data. PMN occurs in the context of NV junctions (stage I) and begins with a bulge in the nuclear envelope (stage II) that develops into a thin-necked bleb (stage III). Bulges in the nuclear envelope are relatively common in TEM thin sections and may not always develop into blebs. A key stage in PMN is the release of vesicles into the lumen of the vacuole (stage IV), after which it is unlikely, but not impossible, that the process can be reversed. Finally, PMN vesicles are degraded (stage V), and their constituent parts are either stored in the vacuole or recycled to the cytoplasm. Importantly, the NV junction apparatus, including Vac8p and Nvj1p, is degraded along with the nucleoplasmic contents of the bleb.

Microautophagy is defined as the delivery of substrates to the vacuole lumen by direct invagination and scission of the vacuole membrane. Because PMN occurs at NV junctions, and Nvj1p-EYFP–associated PMN structures colocalize with FM4-64–stained vacuole membranes, which accumulate in *pep4-Δ* cells, we conclude that PMN is a bona fide form of microautophagy. The selectivity of PMN for the nucleus is determined by interactions between Vac8p in the vacuole
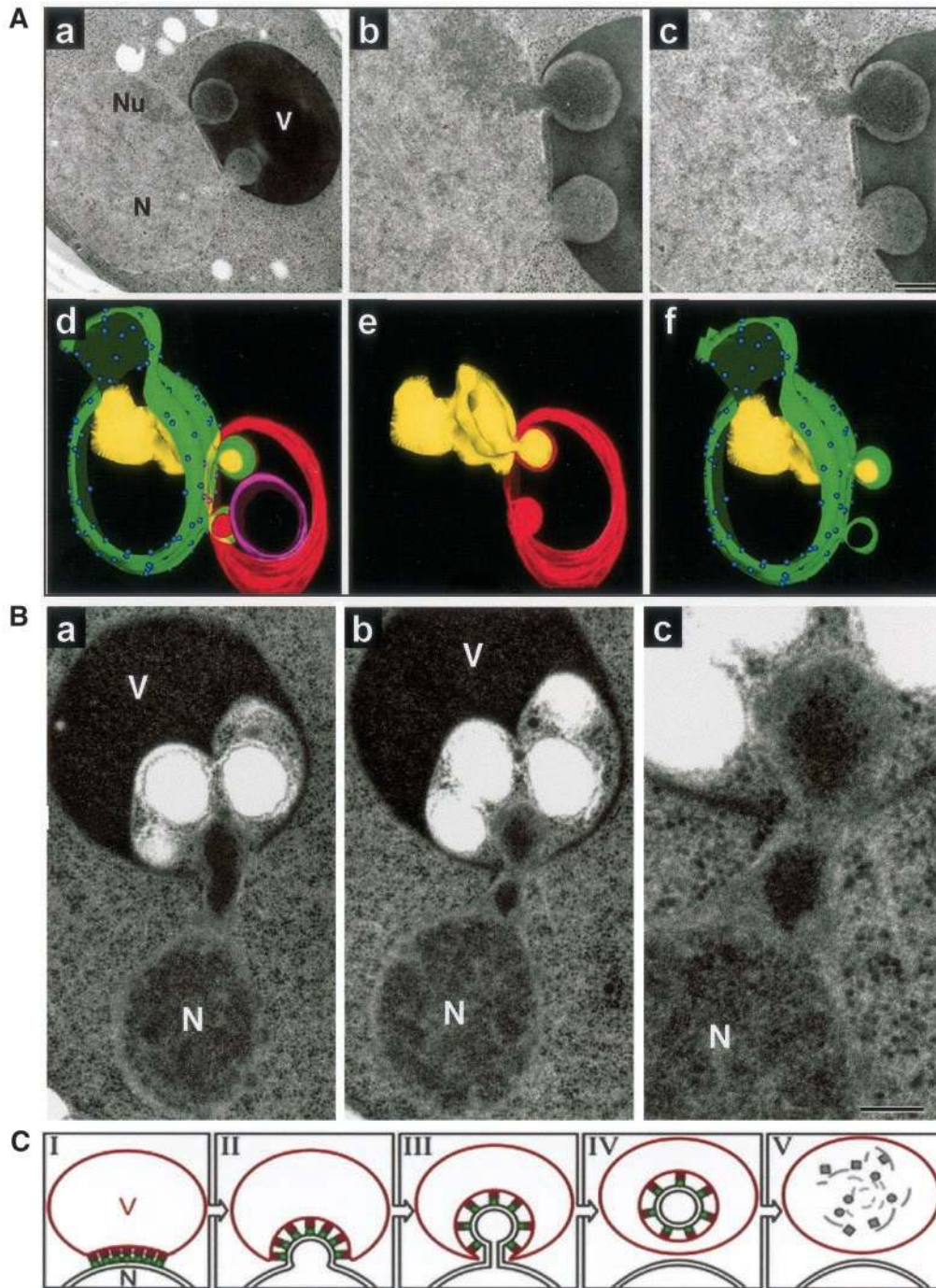
Figure 7. Partitioning of the granular nucleolus into nuclear envelope blebs and a model for PMN. (A) Thin sections of a cell containing two nuclear envelope blebs (a–c). Nucleus (N), nucleolus (Nu), vacuole (V). Three-dimensional reconstruction (d–f) from serial thin sections of the cell shown in panels a-c. Nuclear envelope (green), nuclear pore complexes (blue spheres), nucleolus (yellow), vacuole membrane (red), and an intravacuolar vesicle of unknown origin (magenta). (B) a–c, PMN blebs containing highly condensed material, which may or may not have a nucleolar origin, within the neck and bulb of an elongated bleb that protrudes into a section of the vacuole containing other intravacuolar vesicles. *myo1-Δ* cells were grown to early log phase in SCGlu and transferred to SD-N for 3 h before cryofixation and TEM (see MATERIALS AND METHODS). (C) Model for PMN based on observed structures (stage I). NV junctions are formed by the interaction and clustering of Nvj1p (green circles) in the nuclear envelope with Vac8p (red squares) in the vacuolar membrane (N, nucleus; V, vacuole). Nuclear bulges (stage II) develop into tethered blebs (stage III). Bulging and blebbing could be considered to be early and late steps of the same stage. Intravacuolar vesicles are formed by scission of the vacuolar and two nuclear envelope membranes of the blebs and the release of intravacuolar vesicles into the vacuole lumen (stage IV). Finally, the PMN vesicle and its contents are degraded by vacuolar hydrolases (stage V).

membrane and Nvj1p in the nuclear envelope (Pan *et al.*, 2000). The present results do not limit the physiological function(s) of NV junctions to PMN. For example, NV junctions could play a role in lipid metabolism such as that which occurs between ER and mitochondrial membranes (Achleitner *et al.*, 1999). This notion is supported by reports that enzymes with roles in lipid metabolism concentrate in NV junctions (Kohlwein *et al.*, 2001; Levine and Munro, 2001).

Nucleolar preribosomes are a logical substrate for autophagy. The steady-state cellular concentration of ribosomes and their synthesis are tightly regulated by nutrient limitation. During the period of asynchronous growth when PMN levels rise from ∼5 to ∼35%, the total number of cytoplasmic ribosomes per cell decreases threefold (Ju and Warner, 1994). PMN offers starving cells a handy mechanism for the bulk degradation and recycling of nucleolar preribosomes that are no longer needed in the cytoplasm. The induction of PMN by rapamycin in rapidly dividing cells in rich medium indicates that it is normally under the physiological control of Tor signaling. Inhibition of Tor kinases also arrests prerRNA processing and transiently stabilizes prerRNA precursors in the nucleolus (Powers and Walter, 1999). Thus, Tor may coordinate the arrest of ribosome biogenesis with the degradation of excess ribosomes and preribosomes. We can only speculate about the mechanisms that govern the selection and transport of granular nucleolar material into PMN blebs. Interestingly, the nucleolar material being partitioned into blebs sometimes seems to be more concentrated than the adjacent nucleolus. This phenomenon could be related to the fact that nucleoli are prone to stress-induced aggregation and remodeling (Pelham, 1984; Welch and Suhan, 1986; Webster and Watson, 1993; Tani *et al.*, 1996).

Macroautophagy genes are not required for growth on rich medium but are required for survival in starvation media (Klionsky and Ohsumi, 1999; Ohsumi, 1999). Thus, we were surprised that *nvj1-Δ* cells were no less viable than wt cells after extended periods in SD-N medium. Because the nonessential portion of the nucleus represents only a small fraction of cellular biomass, the selective advantage conferred on cells by PMN in the wild may be too small to detect in the laboratory. Parenthetically, the likelihood that only a portion of the cell's nucleoplasm is degraded by PMN in a reasonable time frame, confounded our attempts to develop a quantitative biochemical assay for the process. Ultimately, Nvj1p-EYFP, whose localization is restricted to NV junctions and is a component of every PMN vesicle, proved a suitable substrate for quantifying rates of degradation by PMN in wt and mutant cells. The lack of a requirement for PMN during starvation could also be due to the existence of redundant degradation pathways. The fact that Nvj1p-EYFP is somewhat unstable in starved *vac8-Δ* cells (15% degradation after 20 h; Figure 6B), indicates that other pathways can degrade integral membrane proteins of the outer nuclear membrane. Proteolysis by nuclear proteasomes (Russell *et al.*, 1999) and RNA hydrolysis by the exosome (van Hoof and Parker, 1999) may be suffice in the absence of PMN.

Apg7p-mediated ubiquitin-like conjugation reactions are required for the formation of autophagosomes in a compartment called the preautophagosomal structure (Abeliovich *et al.*, 2000; Kim *et al.*, 2001a,b). Because microautophagy oc-

curs by invagination, which does not involve autophagosome-like vesicular intermediates, it is unclear what role these reactions might play in microautophagy. For example, proteins involved in the docking/fusion of vesicles with the vacuole are required for macroautophagy but not microautophagy (Darsow *et al.*, 1997; Sato *et al.*, 1998; Sattler and Mayer, 2000). We observed that PMN occurs normally in *apg7-Δ* cells, which are completely defective in Cvt targeting and macroautophagy. Specifically, Nvj1p-EYFP is targeted to FM4-64–stained intravacuolar vesicles at wt levels, and is degraded at wt rates in *apg7-Δ* cells. Yet, micropexophagy and microautophagic tube formation were reported to be at least partially defective in cells deficient in *APG7*-dependent reactions (Yuan *et al.*, 1999; Muller *et al.*, 2000; Sattler and Mayer, 2000; Mukaiyama *et al.*, 2002). Although there could be subtle quantitative defects in PMN in *apg7-Δ* cells, for example, owing to defects in vacuole membrane homeostasis (Sattler and Mayer, 2000), it is clear that the ubiquitin-like conjugation reactions that are absolutely required for autophagosome formation do not play an essential role in PMN.

In conclusion, our findings indicate that PMN is a form of microautophagy that functions to degrade and recycle portions of the nucleus without killing the cell. Questions remain as to whether NV junctions are randomly or selectively positioned on the surface of the nucleus, and how the involvement of the vacuole membrane and both nuclear membranes are coordinated in space and time. The mechanism of nuclear envelope scission during PMN is another interesting event that also occurs during mitosis in yeast. Finally, the study of PMN provides a genetic system for investigating aspects of microautophagy that are conserved in higher eukaryotes.

ACKNOWLEDGMENTS

REFERENCES

Abeliovich, H., Darsow, T., and Emr, S.D. (1999). Cytoplasm to vacuole trafficking of aminopeptidase I requires a t-SNARE-Sec1p complex composed of Tlg2p and Vps45p. EMBO J. *18*, 6005–6016.

Abeliovich, H., Dunn, Jr., W.A., Kim, J., and Klionsky, D.J. (2000). Dissection of autophagosome biogenesis into distinct nucleation and expansion steps. J. Cell Biol. *151*, 1025–1034.

Achleitner, G., Gaigg, B., Krasser, A., Kainersdorfer, E., Kohlwein, S.D., Perktold, A., Zellnig, G., and Daum, G. (1999). Association between the endoplasmic reticulum and mitochondria of yeast facilitates interorganelle transport of phospholipids through membrane contact. Eur. J. Biochem. *264*, 545–553.

Baba, M., Takeshige, K., Baba, N., and Ohsumi, Y. (1994). Ultrastructural analysis of the autophagic process in yeast: detection of autophagosomes and their characterization. J. Cell Biol. *124*, 903–913.

Darsow, T., Rieder, S.E., and Emr, S.D. (1997). A multispecificity syntaxin homologue, Vam3p, essential for autophagic and biosynthetic protein transport to the vacuole. J. Cell Biol. *138*, 517–529.

DeRisi, J.L., Iyer, V.R., and Brown, P.O. (1997). Exploring the metabolic and genetic control of gene expression on a genomic scale. Science *278*, 680–686.

Fleckenstein, D., Rohde, M., Klionsky, D.J., and Rudiger, M. (1998). Yel013p (Vac8p), an armadillo repeat protein related to plakoglobin and importin alpha is associated with the yeast vacuole membrane. J. Cell Sci. *111*, 3109–3118.

Gasch, A.P., Spellman, P.T., Kao, C.M., Carmel-Harel, O., Eisen, M.B., Storz, G., Botstein, D., and Brown, P.O. (2000). Genomic expression programs in the response of yeast cells to environmental changes. Mol. Biol. Cell *11*, 4241–4257.

Guldener, U., Heck, S., Fielder, T., Beinhauer, J., and Hegemann, J.H. (1996). A new efficient gene disruption cassette for repeated use in budding yeast. Nucleic Acids Res. *24*, 2519–2524.

Hardwick, J.S., Kuruvilla, F.G., Tong, J.K., Shamji, A.F., and Schreiber, S.L. (1999). Rapamycin-modulated transcription defines the subset of nutrient-sensitive signaling pathways directly controlled by the Tor proteins. Proc. Natl. Acad. Sci. USA *96*, 14866–14870.

Hutchins, M.U., Veenhuis, M., and Klionsky, D.J. (1999). Peroxisome degradation in *Saccharomyces cerevisiae* is dependent on machinery of macroautophagy and the Cvt pathway. J. Cell Sci. *112*, 4079–4087.

Ichimura, Y., *et al.* (2000). A ubiquitin-like system mediates protein lipidation. Nature *408*, 488–492.

Jones, E.W., Webb, G.C., and Hiller, M.A. (1997). Biogenesis and function of the yeast vacuole. In: The Molecular and Cellular Biology of the Yeast Saccharomyces: Cell Cycle and Cell Biology, ed. J.R. Pringle, J.R. Broach, and E.W. Jones, Cold Spring Harbor, NY: Cold Spring Harbor Laboratory, 363–470.

Jones, E.W., Zubenko, G.S., and Parker, R.R. (1982). PEP4 gene function is required for expression of several vacuolar hydrolases in *Saccharomyces cerevisiae*. Genetics *102*, 665–677.

Ju, Q., and Warner, J.R. (1994). Ribosome synthesis during the growth cycle of *Saccharomyces cerevisiae*. Yeast *10*, 151–157.

Kamada, Y., Funakoshi, T., Shintani, T., Nagano, K., Ohsumi, M., and Ohsumi, Y. (2000). Tor-mediated induction of autophagy via an Apg1 protein kinase complex. J. Cell Biol. *150*, 1507–1513.

Kim, J., Huang, W.P., and Klionsky, D.J. (2001a). Membrane recruitment of Aut7p in the autophagy and cytoplasm to vacuole targeting pathways requires Aut1p, Aut2p, and the autophagy conjugation complex. J. Cell Biol. *152*, 51–64.

Kim, J., Huang, W.P., Stromhaug, P.E., and Klionsky, D.J. (2001b). Convergence of multiple autophagy and Cvt components to a perivacuolar membrane compartment prior to De Novo vesicle formation. J. Biol. Chem. *23*, 23.

Klionsky, D.J., and Ohsumi, Y. (1999). Vacuolar import of proteins and organelles from the cytoplasm. Annu. Rev. Cell. Dev. Biol. *15*, 1–32.

Kohlwein, S.D., Eder, S., Oh, C.S., Martin, C.E., Gable, K., Bacikova, D., and Dunn, T. (2001). Tsc13p is required for fatty acid elongation and localizes to a novel structure at the nuclear-vacuolar interface in *Saccharomyces cerevisiae*. Mol. Cell. Biol. *21*, 109–125.

Kremer, J.R., Mastronarde, D.N., and McIntosh, J.R. (1996). Computer visualization of three-dimensional image data using IMOD. J. Struct. Biol. *116*, 71–76.

Leger-Silvestre, I., Trumtel, S., Noaillac-Depeyre, J., and Gas, N. (1999). Functional compartmentalization of the nucleus in the budding yeast *Saccharomyces cerevisiae*. Chromosoma *108*, 103–113.

Levine, T.P., and Munro, S. (2001). Dual targeting of Osh1p, a yeast homologue of oxysterol-binding protein, to both the Golgi and the nucleus-vacuole junction. Mol. Biol. Cell *12*, 1633–1644.

Mizushima, N., Noda, T., Yoshimori, T., Tanaka, Y., Ishii, T., George, M.D., Klionsky, D.J., Ohsumi, M., and Ohsumi, Y. (1998a). A protein conjugation system essential for autophagy. Nature *395*, 395–398.

Mizushima, N., Sugita, H., Yoshimori, T., and Ohsumi, Y. (1998b). A new protein conjugation system in human. The counterpart of the yeast Apg12p conjugation system essential for autophagy. J. Biol. Chem. *273*, 33889–33892.

Moskvina, E., Schuller, C., Maurer, C.T., Mager, W.H., and Ruis, H. (1998). A search in the genome of *Saccharomyces cerevisiae* for genes regulated via stress response elements. Yeast *14*, 1041–1050.

Mukaiyama, H., Oku, M., Baba, M., Samizo, T., Hammond, A.T., Glick, B.S., Kato, N., and Sakai, Y. (2002). Paz2 and 13 other PAZ gene products regulate vacuolar engulfment of peroxisomes during micropexophagy. Genes Cells *7*, 75–90.

Muller, O., Sattler, T., Flotenmeyer, M., Schwarz, H., Plattner, H., and Mayer, A. (2000). Autophagic tubes: vacuolar invaginations involved in lateral membrane sorting and inverse vesicle budding. J. Cell Biol. *151*, 519–528.

Noda, T., Matsuura, A., Wada, Y., and Ohsumi, Y. (1995). Novel system for monitoring autophagy in the yeast *Saccharomyces cerevisiae*. Biochem. Biophys. Res. Commun. *210*, 126–132.

Noda, T., and Ohsumi, Y. (1998). Tor, a phosphatidylinositol kinase homologue, controls autophagy in yeast. J. Biol. Chem. *273*, 3963–3966.

Noda, T., Suzuki, K., and Ohsumi, Y. (2002). Yeast autophagosomes: de novo formation of a membrane structure. Trends Cell Biol. *12*, 231–235.

Ohsumi, Y. (1999). Molecular mechanism of autophagy in yeast, *Saccharomyces cerevisiae. Phil. Trans. R. Soc. Lond. B Biol. Sci. 354*, 1577–1580; discussion 1580–1571.

Pan, X., and Goldfarb, D.S. (1998). YEB3/VAC8 encodes a myristylated armadillo protein of the *Saccharomyces cerevisiae* vacuolar membrane that functions in vacuole fusion and inheritance. J. Cell Sci. *111*, 2137–2147.

Pan, X., Roberts, P., Chen, Y., Kvam, E., Shulga, N., Huang, K., Lemmon, S., and Goldfarb, D.S. (2000). Nucleus-vacuole junctions in *Saccharomyces cerevisiae* are formed through the direct interaction of Vac8p with Nvj1p. Mol. Biol. Cell *11*, 2445–2457.

Pelham, H.R. (1984). Hsp70 accelerates the recovery of nucleolar morphology after heat shock. EMBO J. *3*, 3095–3100.

Powers, T., and Walter, P. (1999). Regulation of ribosome biogenesis by the rapamycin-sensitive TOR-signaling pathway in *Saccharomyces cerevisiae*. Mol. Biol. Cell *10*, 987–1000.

Russell, S.J., Steger, K.A., and Johnston, S.A. (1999). Subcellular localization, stoichiometry, and protein levels of 26 S proteasome subunits in yeast. J. Biol. Chem. *274*, 21943–21952.

Sakai, Y., Koller, A., Rangell, L.K., Keller, G.A., and Subramani, S. (1998). Peroxisome degradation by microautophagy in *Pichia pastoris*: identification of specific steps and morphological intermediates. J. Cell Biol. *141*, 625–636.

Sato, T.K., Darsow, T., and Emr, S.D. (1998). Vam7p, a SNAP-25-like molecule, and Vam3p, a syntaxin homolog, function together in yeast vacuolar protein trafficking. Mol. Cell. Biol. *18*, 5308–5319.

Sattler, T., and Mayer, A. (2000). Cell-free reconstitution of micro-autophagic vacuole invagination and vesicle formation. J. Cell Biol. *151*, 529–538.

Scott, S.V., Hefner-Gravink, A., Morano, K.A., Noda, T., Ohsumi, Y., and Klionsky, D.J. (1996). Cytoplasm-to-vacuole targeting and autophagy employ the same machinery to deliver proteins to the yeast vacuole. Proc. Natl. Acad. Sci. USA *93*, 12304–12308.

Scott, S.V., Nice, D.C. 3rd, Nau, J.J., Weisman, L.S., Kamada, Y., Keizer-Gunnink, I., Funakoshi, T., Veenhuis, M., Ohsumi, Y., and Klionsky, D.J. (2000). Apg13p and Vac8p are part of a complex of phosphoproteins that are required for cytoplasm to vacuole targeting. J. Biol. Chem. *275*, 25840–25849.

Severs, N.J., Jordan, E.G., and Williamson, D.H. (1976). Nuclear pore absence from areas of close association between nucleus and vacuole in synchronous yeast cultures. J. Ultrastruct. Res *54*, 374–387.

Sherman, F. (1991). Getting started with yeast. Methods Enzymol. *194*, 3–21.

Suzuki, K., Kirisako, T., Kamada, Y., Mizushima, N., Noda, T., and Ohsumi, Y. (2001). The pre-autophagosomal structure organized by concerted functions of APG genes is essential for autophagosome formation. EMBO J. *20*, 5971–5981.

Takeshige, K., Baba, M., Tsuboi, S., Noda, T., and Ohsumi, Y. (1992). Autophagy in yeast demonstrated with proteinase-deficient mutants and conditions for its induction. J. Cell Biol. *119*, 301–311.

Tani, T., Derby, R.J., Hiraoka, Y., and Spector, D.L. (1996). Nucleolar accumulation of poly (A)+ RNA in heat-shocked yeast cells: implication of nucleolar involvement in mRNA transport. Mol. Biol. Cell *7*, 173–192.

Teter, S.A., and Klionsky, D.J. (2000). Transport of proteins to the yeast vacuole: autophagy, cytoplasm-to-vacuole targeting, and role of the vacuole in degradation. Semin. Cell. Dev. Biol. *11*, 173–179.

Tuttle, D.L., and Dunn, W.A. Jr. (1995). Divergent modes of autophagy in the methylotrophic yeast *Pichia pastoris*. J. Cell Sci. *108*, 25–35.

van Hoof, A., and Parker, R. (1999). The exosome: a proteasome for RNA? Cell *99*, 347–350.

Veit, M., Laage, R., Dietrich, L., Wang, L., and Ungermann, C. (2001). Vac8p release from the SNARE complex and its palmitoylation are coupled and essential for vacuole fusion. EMBO J. *20*, 3145–3155.

Wach, A. (1996). PCR-synthesis of marker cassettes with long flanking homology regions for gene disruptions in *S. cerevisiae*. Yeast *12*, 259–265.

Wang, Y.X., Catlett, N.L., and Weisman, L.S. (1998). Vac8p, a vacuolar protein with armadillo repeats, functions in both vacuole inheritance and protein targeting from the cytoplasm to vacuole. J. Cell Biol. *140*, 1063–1074.

Wang, Y.X., Zhao, H., Harding, T.M., Gomes de Mesquita, D.S., Woldringh, C.L., Klionsky, D.J., Munn, A.L., and Weisman, L.S. (1996). Multiple classes of yeast mutants are defective in vacuole partitioning yet target vacuole proteins correctly. Mol. Biol. Cell *7*, 1375–1389.

Webster, D.L., and Watson, K. (1993). Ultrastructural changes in yeast following heat shock and recovery. Yeast *9*, 1165–1175.

Welch, W.J., and Suhan, J.P. (1986). Cellular and biochemical events in mammalian cells during and after recovery from physiological stress. J. Cell Biol. *103*, 2035–2052.

Winey, M., Mamay, C.L., O'Toole, E.T., Mastronarde, D.N., Giddings, T.H. Jr., McDonald, K.L., and McIntosh, J.R. (1995). Three-dimensional ultrastructural analysis of the *Saccharomyces cerevisiae* mitotic spindle. J. Cell Biol. *129*, 1601–1615.

Woolford, C.A., Noble, J.A., Garman, J.D., Tam, M.F., Innis, M.A., and Jones, E.W. (1993). Phenotypic analysis of proteinase A mutants. Implications for autoactivation and the maturation pathway of the vacuolar hydrolases of *Saccharomyces cerevisiae*. J. Biol. Chem. *268*, 8990–8998.

Yuan, W., Stromhaug, P.E., and Dunn, W.A. Jr. (1999). Glucose-induced autophagy of peroxisomes in *Pichia pastoris* requires a unique E1-like protein. Mol. Biol. Cell *10*, 1353–1366.

Zubenko, G.S., Park, F.J., and Jones, E.W. (1983). Mutations in PEP4 locus of *Saccharomyces cerevisiae* block final step in maturation of two vacuolar hydrolases. Proc. Natl. Acad. Sci. USA *80*, 510–514.